PPARα protects against *trans*-fatty acid-containing diet-induced steatohepatitis

Xiao Hu [1], Naoki Tanaka[1], Ran Guo [1], Yu Lu [1], Takero Nakajima[1], Frank J. Gonzalez[2], and Toshifumi Aoyama[1]

[1]Department of Metabolic Regulation, Shinshu University Graduate School of Medicine, Matsumoto, Japan

[2]Laboratory of Metabolism, Center for Cancer Research, National Cancer Institute, National Institutes of Health, Bethesda, MD

Correspondence: Naoki Tanaka, M.D., Ph. D. Department of Metabolic Regulation, Shinshu University Graduate School of Medicine, 390-8621, Matsumoto, Japan
E-mail: naopi@shinshu-u.ac.jp; Tel: +81-263-37-2851

Running title: PPARα protects liver from dietary *trans*-fatty acid

Manuscript length: Total words 2590; Abstract words 241; Title (characters with spaces) 97

Numbers of Figures and Tables: 7 figures and supplementary data (1 figure and 3 tables)

Potential conflict of interest: The authors have declared that no conflict of interest exists.

Financial support: The authors have declared that no financial support exists.

Abbreviations:

ACCα, acetyl-coenzyme A carboxylase α; ALT, alanine aminotransferase; ATGL, adipose triglyceride lipase; ER, endoplasmic reticulum; FA, fatty acid; FABP1, FA-binding protein 1; FAS, FA synthase; IL, interleukin; LACS, long-chain

acyl-coenzyme A synthase; LCAD, long-chain acetyl-CoA dehydrogenase; MCP1, monocyte chemoattractant protein 1; MTP, microsomal TG transfer protein; NAFLD, non-alcoholic fatty liver disease; NASH, non-alcoholic steatohepatitis; NF-κB, nuclear factor-kappa B; OPN, osteopotin; PPAR, peroxisome proliferator-activated receptor; qPCR, quantitative polymerase chain reaction; TFA, *trans*-fatty acid; TG, triglyceride; TLR, toll-like receptor; TNFα, tumor necrosis factor α; VLCAD, very-long-chain acetyl-CoA dehydrogenase.

Abstract

Consumption of *trans*-fatty acids (TFA), unsaturated fatty acids (FA) containing *trans* double bonds, is a risk factor for metabolic syndrome and steatohepatitis. Peroxisome proliferator-activated receptor α (PPARα) is a master regulator of hepatic lipid homeostasis. To examine the contribution of PPARα to changes in liver phenotypes induced by TFA, two diets were used: a purified control diet and an isocaloric diet in which most of the soybean oil, a major source of FA in the diet, was replaced with TFA-rich shortening. The diets were fed to wild-type and *Ppara*-null mice for two months. *Ppara*-null mice fed a TFA-containing diet showed more severe hepatic steatosis and liver damage compared with similarly-treated wild-type mice, as revealed by increased hepatic triglyceride (TG) contents and serum alanine aminotransferase activities. While the TFA diet increased the hepatic expression of enzymes involved in *de novo* FA synthesis and decreased TG-hydrolyzing enzymes in both genotypes, the expression of FA-catabolizing enzymes were decreased in *Ppara*-null mice, resulting in more severe hepatosteatosis. Additionally, the expression levels of key contributors to inflammation, such as osteopontin, were increased, and nuclear factor-kappa B was activated in TFA-containing diet-fed *Ppara*-null mice. Enhanced inflammatory signaling in these mice was presumably mediated by toll-like receptor 2, with no accompanying inflammasome activation. Collectively, these results suggest a protective role for PPARα in the pathological changes in the liver following TFA consumption. PPARα might prevent TFA-induced steatohepatitis.

(229 words)

Key Words: *trans*-fatty acid, PPARα, nuclear factor-kappa B, osteopontin, toll-like receptor, inflammasome

Highlights:

1. **The role of PPARα in trans-fatty acid (TFA)-induced liver abnormalities remains unclear.**
2. **TFA-fed *Ppara*-null mice showed more severe hepatosteatosis and liver damage.**
3. **Suppressed lipolysis/β-oxidation caused severe steatosis in these mice.**
4. **Toll-like receptor 2-mediated inflammatory signaling likely caused liver injury.**
5. **A preventive effect of PPARα on TFA-induced steatohepatitis was shown.**

1. Introduction

Unsaturated fatty acids (FA) generally have two forms of double bonds, *cis* and *trans*. In *cis*-FA, the two carbon atoms forming double bonds bind two hydrogen atoms on the same side, leading to a curved space conformation. However, the two carbon atoms of the double bonds in *trans*-FA (TFA) bind two hydrogen atoms on the diagonal side of the carbon chain, resulting in a linear conformation [1]. Although natural foods, such as animal meat or dairy products, contain very few natural TFA, large amounts of TFA are detected in shortening, bread, margarine, cream cakes, fried fast food and some other processed foods. Partially hydrogenated vegetable oils are often used by the food industry to enhance the stability and palatability of foods, and TFA are produced by the partial hydrogenation of vegetable oils [1, 2]. Therefore, TFA are recognized as an artificial lipid closely associated with dietary habits in developed countries.

It was reported that TFA are more harmful to humans than other FA. Notably, TFA increase blood viscosity, leading to thrombosis and elevates circulating low-density-lipoprotein cholesterol and decreases high-density-lipoprotein cholesterol, promoting arteriosclerosis and coronary heart disease [3, 4]. Additionally, several clinical studies demonstrated the possible association between excessive TFA intake and metabolic syndrome, insulin resistance, obesity, Alzheimer's disease, depression, and infertility [5-8]. Therefore, in North American and European countries, governments have enacted legislation to require the food processing industry to stop using TFA in food production. However, in Asia, TFA is still widely used in processed foods [9].

Non-alcoholic fatty liver disease (NAFLD) is a chronic liver disorder that is increasing worldwide and its progressive subtype, non-alcoholic steatohepatitis (NASH), can eventually develop into cirrhosis and/or hepatocellular carcinoma [10-12]. Several key factors, such as lipotoxicity, oxidative stress, aberrant immune system, and inflammatory signaling, are known to contribute to the progression from steatosis to steatohepatitis. For example, toll-like receptors (TLRs) recognize a variety of pathogen-associated molecular patterns, activating immune responses [13]. The

fact that disruption of TLR2 or TLR4 attenuated NASH phenotypes indicated a crucial role of TLR-mediated signaling in the pathogenesis of NAFLD/NASH [14]. Additionally, up-regulation of pro-inflammatory mediators, such as tumor necrosis factor α (TNFα), monocyte chemoattractant protein 1 (MCP1), and osteopontin (OPN), are closely associated with several types of liver injury [15]. The mechanism of NASH is multifactorial and complicated.

Some studies have shown that high TFA intake promotes fatty acid/triglyceride (FA/TG) synthesis, decreases TG export and inhibits FA β-oxidation, leading to hepatosteatosis [16, 17]. Since high TFA consumption induces enhanced pro-inflammatory cytokine levels and microcirculatory disturbances resulting in hepatic inflammation [16, 18, 19], excessive dietary TFA may play an important role in the development of NAFLD/NASH.

Peroxisome proliferator-activated receptor α (PPARα) is a ligand-activated nuclear receptor that regulates lipid transport and catabolism and also influences inflammation and immune responses [20-23]. However, the role of PPARα in TFA-induced liver abnormalities remains unclear. In the present study, wild-type and *Ppara*-null mice were treated for two months with a control diet or an isocaloric diet where most of the FA are replaced with TFA, and liver phenotypes were examined.

2. Methods

2.1. Mice and treatment

All animal experiments were conducted in accordance with animal study protocols outlined in the "Guide for the Care and Use of Laboratory Animals" prepared by the National Academy of Sciences and approved by Shinshu University School of Medicine. *Ppara*-null mice on a Sv/129 genetic background and the wild-type counterparts were maintained under controlled conditions (25 ^{o}C; 12h light/dark cycle) with tap water and standard laboratory chow *ab libitum*. Male 10- to 14-week-old wild-type and *Ppara*-null mice weighing 25-35 g were selected and each genotype was divided into two groups (n= 3-6/group) [20, 23]. To eliminate the effect of high fat/calorie due to adding TFA and avoid essential FA deficiency, 60 g of soybean oil (70 g in total in 1000 g of purified AIN93G diet) was replaced by the same weight of Primex^{R}, a regular shortening containing large amount of TFA. The TFA-containing diet and control AIN93G diet were made by Research Diets, Inc. (New Brunswick, NJ: #D14020301 and D10012G, respectively); detailed nutrient/FA composition of the diets shown in Supplementary Table 1 and 2, respectively. Calorie per weight in the TFA-containing diet was identical to that in AIN93G diet. As such, one group in each genotype was treated with the isocaloric TFA-containing AIN93G diet and the other group was given the control AIN93G diet for two months. After the treatment, the mice were anesthesized and killed by CO_2 asphyxiation at 6 hours after food withdrawal, and blood and tissues collected. Blood was centrifuged at 3,000 rpm for 15 minutes twice and the serum was collected. Sera and tissues were immediately frozen and kept in -80 ^{o}C freezer until used.

2.2. Biochemical analysis

Serum alanine aminotransferase (ALT), TG, total cholesterol, non-esterified FA, phospholipid, and glucose were measured with enzyme assay kits (Wako Pure Chemical Industries, Ltd., Osaka, Japan). Liver lipids were extracted by hexane: isopropanol method as described previously and measured using enzymatic assay kits (Wako Pure Chemical Industries) [24].

2.3. Histological analysis

Liver tissue was fixed in 10% neutral formalin, embedded in paraffin, cut into 4-μm sections, and stained with the hematoxylin and eosin dyes [25].

2.4. Analysis of mRNA expression

Total liver RNA was extracted using an RNeasy Mini Kit (Qiagen, Tokyo, Japan), and reverse-transcribed to cDNA using oligo-dT and random primers with SuperScript II reverse transcriptase (Invitrogen Corporation, Carlsbad, CA). Levels of mRNA were measured by quantitative real-time polymerase chain reactions (qPCR) using an SYBR Premix Ex Taq II (Takara Bio, Otsu, Japan) on a Thermal Cycler Dice TP800 system (Takara Bio). The mRNA encoding glyceraldehyde-3-phosphate dehydrogenase (*Gapdh*) was used as an internal control. Sequences of primers are shown in Supplementary Table 3 [26, 27]. The mRNA levels were normalized to *Gapdh* mRNA levels and expressed as a fold change relative to those of wild-type mice fed a control diet.

2.5. Immunoblot analysis

Preparation of whole liver homogenates was conducted as described previously [20-23, 28] and liver nuclear fractions were isolated with NE-PER Nuclear and Cytoplasmic Extraction Reagents (Thermo Fisher Scientific, Rockford, IL). Protein concentrations were measured colorimetrically with the BCA Protein Assay kit (Pierce, Rockford, IL, USA). Whole liver homogenates (20-60 μg of protein in each lane) were separated using sodium dodecyl sulfate-polyacrylamide gel electrophoresis (SDS-PAGE). The polyacrylamide concentration in the gel was 6%, 10%, or 12.5%, which was dependent on molecular weight of the target protein. For analysis of the nuclear factor-kappa B (NF-κB) p65 component, nuclear proteins (30 μg in each lane) were subjected to 10% SDS-PAGE. After electrophoresis, the proteins were transferred to a nitrocellulose filter membrane (Amersham Hybond-P, GE Health Care, Little Chalfont, UK). The membranes were blocked for 1 hour with 5% bovine

serum albumin or 5% non-fat dry milk in Tris-buffered saline and incubated overnight with the respective primary antibody. Primary antibodies against FA-binding protein 1 (FABP1), long-chain acyl-coenzyme A (CoA) synthase (LACS), and long-chain and very-long-chain acetyl-CoA dehydrogenase (LCAD and VLCAD, respectively) were described previously [29]. The following primary antibodies were purchased from Santa Cruz Biotechnology (Dallas, TX): FA synthase (FAS), #16147, 1:200 dilution; acetyl-CoA carboxylase α (ACCα), #30212, 1:200 dilution; CD36, #9154, 1:200 dilution; microsomal TG transfer protein (MTP), #33116, 1:200 dilution; and histone H1, #10806, 1:200 dilution. The following primary antibodies were purchased from Cell Signaling Technology (Denver, MA): adipose TG lipase (ATGL), #2439, 1:1000 dilution; TLR2, #13744, 1:1000 dilution [25, 26]; and p65, #8242, 1:1000 dilution. The antibody against OPN and β-actin were obtained from Abcam (Cambridge, MA): OPN, #8448, 1:1000 dilution and β-actin, #8227, 1:1000 dilution. After four washes, the membranes were incubated with alkaline phosphatase-conjugated secondary antibodies (Jackson ImmunoResearch Laboratories, West Grove, PA, #93785, 1:1000 dilution) and treated with 1-step NBT/BCIP substrate (Pierce, Rockford, IL). The true band positions were determined by co-electrophoresing molecular weight standards (Bio-Rad, Hercules, CA) and the band of β-actin or histone H1 was used as a loading control. Immunoblotting was repeated twice for each protein and each band intensity was quantified using NIH image J (National Institutes of Health, Bethesda, MD), normalized by those of loading control, and subsequently expressed as a fold change relative to those of wild-type mice fed a control diet.

2.6. Statistical analysis

Results are expressed as mean ± standard error of the mean (SEM). Statistical analysis was performed using two-way ANOVA with Bonferroni's correction. A *P* value of less than 0.05 was considered to be statistically significant.

3. Results

3.1. TFA-containing diet-fed Ppara-null mice develop more severe hepatic steatosis and inflammation compared with the wild-type mice

Wild-type and *Ppara*-null mice were examined two months after commencing TFA-containing diet treatment, revealing that enlarged and yellowish livers were seen only in *Ppara*-null mice. While body weight and epididymal fat pad weight were similar between the groups, liver weights showed a significant increase in *Ppara*-null mice treated with the TFA diet compared with similarly-treated wild-type mice (Fig. 1A). In these mice, serum ALT levels, indicators of liver injury, were significantly increased in TFA diet-fed *Ppara*-null mice (Fig. 1B). Serum TG was also increased in TFA diet-treated *Ppara*-null mice compared with control diet-treated *Ppara*-nulls, but the increase did not reach statistical significance compared with TFA diet-fed wild-type mice ($P = 0.08$) (Fig. 1B). Serum levels of glucose, non-esterified FA, and total cholesterol were not different between the groups (data not shown). Hepatic TG contents were significantly increased compared with TFA diet-treated wild-type mice and control diet-fed *Ppara*-null mice (Fig. 1B). Histological analysis of the liver revealed very mild macrovesicular steatosis only in TFA diet-fed wild-type mice. However, in TFA diet-fed *Ppara*-null mice, abundant macrovesicular lipid droplets and inflammatory foci were detected throughout the section (Fig. 1C). These results demonstrate that more severe steatosis and inflammation was observed in *Ppara*-null mice fed the TFA-containing diet than was observed in wild-type mice.

3.2. Reduced FA utilization is associated with steatogenesis in TFA-containing diet-treated Ppara-null mice

To investigate the mechanism of severe hepatosteatosis in TFA-rich diet-fed *Ppara*-null mice, the expression of genes associated with FA and TG metabolism in the liver were measured. The mRNA levels of genes encoding FAS and ACCα (*Fasn* and *Acaca*, respectively), which are involved in *de novo* FA synthesis, were increased after TFA diet treatment in both genotypes with no significant differences between genotypes (Fig. 2A). The mRNA levels of *Cd36*, which plays an important role in FA

uptake from blood, showed significant increases in *Ppara*-null mice compared with wild-type mice in both diets (Fig. 2A). Immunoblot analysis confirmed increased hepatic expression of FAS/ACCα following TFA diet (Fig. 2B and C), indicating enhanced FA synthesis due to TFA-containing diet independently of PPARα.

The mRNA expression of genes encoding FABP1 (*Fabp1*) and LACS (*Acsl1*), which is related to intracellular FA carriage and activation, respectively, was significantly decreased in TFA diet-fed *Ppara*-null mice compared with their similarly-treated wild-type counterparts (Fig. 3A). Decreased expression was also observed for *Acadl* and *Acadvl* mRNAs, which encode the FA-oxidizing enzymes LCAD and VLCAD, respectively (Fig. 3A). These PPARα-dependent changes in FA-eliminating enzymes/proteins were also observed at the protein level (Fig. 3B and C).

There were no significant differences in the mRNA levels of genes related to TG synthesis (*Dgat1* and *Dgat2*, encoding diacylglycerol acyltransferase 1 and 2, respectively) and TG export (*Mttp*, encoding MTP) (Fig. 4A). While the mRNA levels of *Pnpla2* and *Lipe*, encoding TG-hydrolyzing enzymes ATGL and hormone-sensitive lipase, respectively, were decreased after TFA diet administration in both genotypes, there were no significant differences between the wild-type and *Ppara*-null mice (Fig. 4A). Significant down-regulation of ATGL expression in both genotypes after TFA consumption (Fig. 4B and C) suggested that TFA suppressed lipolysis in the liver independently of PPARα.

Overall, although enhanced *de novo* lipogenesis and attenuated lipolysis in the liver were likely associated with TFA consumption, reduced FA utilization was a main cause of more severe steatosis in the TFA-containing diet-fed *Ppara*-null mice.

3.3. Increased hepatic inflammation in TFA-containing diet-treated Ppara-null mice is related to NF-κB activation mainly mediated by toll-like receptor 2, but not by inflammasome

In order to examine the mechanism of more severe hepatitis in TFA-containing diet-fed *Ppara*-null mice, hepatic expression of typical pro-inflammatory mediators

was determined. The mRNA levels of *Tnf* and *Ccl2*, encoding TNFα and MCP1, respectively, were increased in TFA-rich diet-fed *Ppara*-null mice (Fig. 5A). The mRNA levels of *Spp1* and *Col1a1*, encoding OPN and collagen 1a1, respectively, which promote hepatic inflammation/fibrosis, were also increased in these mice (Fig. 5A). Marked up-regulation of OPN was also confirmed at the protein level (Fig. 5B and C). The expression of mRNAs encoded by these key genes is induced by activation of NF-κB [30]. Indeed, increased nuclear p65 levels were detected in TFA-containing diet-administered *Ppara*-null mice compared with wild-type mice (Fig. 5B and C), indicating that NF-κB was activated in the former mice.

NF-κB is activated by several upstream signals, such as oxidative stress, endoplasmic reticulum (ER) stress, inflammasome, and TLR-mediated pathway [30]. The expression of mRNAs encoding reactive oxygen species-generating/eliminating enzymes and ER stress-induced transcription factor were not different between TFA-containing diet-fed wild-type and *Ppara*-null mice (Supplementary Fig. 1). The mRNAs encoded by inflammasome-related genes, such as *Nlrp3*, *Nlrc4*, *Aim2, Pycard, Casp1, and Il1b*, were not increased in TFA diet-treated *Ppara*-null mice (Fig. 6). Alternatively, among the genes associated with the TLR-mediated pathway, *Tlr2* mRNA and TLR2 protein levels were significantly increased in TFA diet-treated *Ppara*-null mice compared with similarly-treated wild-type mice (Fig. 7). Therefore, severe hepatic inflammation observed in TFA-containing diet-treated *Ppara*-null mice is associated with NF-κB activation likely due to enhanced TLR2-mediated signaling.

4. Discussion

TFA is artificially produced in the process of food hydrogenation and is more harmful to the body than naturally-occurring FA [2, 31]. The current study investigated the role of PPARα in TFA-induced liver abnormalities. Previous studies examined the effect of dietary TFA by adding TFA to the regular diet or by using a TFA-rich high-fat diet [16, 17, 32, 33]. However, it is unclear whether the pathological changes induced by a TFA-rich high-fat diet are due to TFA toxicity or the high fat/calorie contents. In the present study, a special isocaloric AIN93G diet was made by replacing most of the soybean oil with shortening containing large amounts of TFA and keeping a minimal amount of essential FA in order to more precisely assess the physiological effects of TFA. The isocaloric TFA-containing diet-fed *Ppara*-null mice had severe steatosis and inflammation, activated NF-κB, and enhanced inflammatory signaling. These results indicate that mice lacking PPARα are more prone to steatohepatitis following TFA consumption, and thus PPARα may protect livers against dietary TFA-induced toxicity.

It was reported that TFA intake enhanced *de novo* lipogenesis [16, 33, 34]. This finding was consistent with results of the present study that hepatic FAS/ACCα expression was increased after TFA-containing diet consumption in both genotypes. Additionally, the expression of TG-hydrolyzing enzymes, i.e., *Pnpla2/Lipe* mRNA and ATGL protein levels, were decreased after the TFA diet. Augmented *de novo* FA synthesis and suppressed lipolysis are likely associated with TFA-induced TG accumulation in the liver. However, remarkable reductions in the expression levels of the proteins involved in intracellular FA transport and FA β-oxidation, such as FABP1, LCAD, and VLCAD, were detected only in *Ppara*-null mice. A significant imbalance between lipogenesis, lipolysis, and FA utilization is likely the main mechanism for steatogenesis in TFA-containing diet-fed *Ppara*-null mice.

Elevated serum ALT, enhanced expression of pro-inflammatory molecules, and liver histology indicated the presence of hepatitis in TFA diet-treated *Ppara*-null mice. NF-κB is a pivotal transcription factor in regulating genes involved in the inflammatory response, and its activation is driven by a wide variety of stimuli, such

as growth factors, cytokines, bacteria/virus, and cellular stress [30, 35]. TLRs are among the key mediators of NF-κB signaling [36]. In mammals, TLR2 and TLR4 were closely associated with the development of steatohepatitis [14, 37] and some studies proposed that certain lipids, such as saturated FA, can activate TLR2 signaling in hepatic Kupffer cells, ultimately leading to NF-κB activation and steatohepatitis [38]. The findings in the present study provide intriguing possibilities that TFA can directly activate TLR2 signaling in hepatocytes/Kupffer cells under the PPARα-deficient state and that PPARα modulates FA-TLR linkage. Future studies to treat TFA with isolated hepatocytes/Kupffer cells from *Ppara*-null mice might be of value to address these questions.

The present study revealed significant increases in OPN expression in the livers of *Ppara*-null mice given the TFA-rich diet. OPN is a Th1 cytokine which plays an important role in the development of various inflammatory and fibrotic diseases [15]. In a mouse model of NASH induced by a methionine- and choline-deficient diet, hepatic OPN expression was markedly and initially increased and its disruption notably attenuated NASH severity [39]. Some studies demonstrated that alterations in hepatocyte metabolism and fat accumulation in the liver facilitate the increases in OPN [40]. Additionally, a recent study observed that TLR2, but not TLR4, up-regulated OPN production [41]. Therefore, OPN may be a key contributor to the development of NASH in TFA-containing diet-fed *Ppara*-null mice.

Inflammasomes, intracellular multiprotein complex, are also major mediators of inflammatory response. Exogenous and endogenous danger signals, such as ATP, cholesterol/uric acid crystal, and lipopolysaccharide, activate caspase-1, which cleaves pro-interleukin (IL)-1β into mature one [42, 43]. It was reported that saturated but not unsaturated FA can active inflammasomes in hepatocytes and induce IL-1β release [44], which may be in accordance with the present results since TFA is structurally classified as an unsaturated FA. The association between inflammasome, TFA, and PPARα needs to be addressed in the future.

Since PPARα is down-regulated with the progression of steatohepatitis [11, 45], the present results suggest that dietary TFA is more harmful to NASH patients, and

that dietary TFA may accelerate NASH progression. Restriction of TFA intake and TFA-rich westernized diets may be useful to attenuate liver injury in NAFLD/NASH patients. Additionally, therapeutic interventions to maintain PPARα function might be beneficial to reduce TFA toxicity.

In conclusion, the present results demonstrate that PPARα disruption is more sensitive to steatohepatitis following TFA consumption, indicating that PPARα plays a protective role for dietary TFA-induced liver abnormalities.

References

[1] Mensink RP, Katan MB. Trans monounsaturated fatty acids in nutrition and their impact on serum lipoprotein levels in man. Prog lipid Res 1993; 32: 111-22.

[2] Sommerfeld M. Trans unsaturated fatty acids in natural products and processed foods. Prog lipid Res 1983; 22: 221-33.

[3] Mozaffarian D, Katan MB. Ascherio A, Stampfer MJ, Willett WC. Trans fatty acids and cardiovascular disease. N Engl J Med 2006; 354: 1601-13.

[4] Mensink RP, Katan MB. Effect of dietary trans fatty acids on high-density and low-density lipoprotein cholesterol levels in healthy subjects. N Engl J Med 1990; 323: 439-45.

[5] Lottenberg AM, Afonso Mda S, Lavrador MS, Machado RM, Nakandakare ER. The role of dietary fatty acids in the pathology of metabolic syndrome. J Nutr Biochem 2012; 23: 1027-40.

[6] Micha R, Mozaffarian D. Trans fatty acids: effects on metabolic syndrome, heart disease and diabetes. Nat Rev Endocrinol 2009; 5: 335-44.

[7] Phivilay A, Julien C, Tremblay C, Berthiaume L, Julien P, Giguère Y, et al. High dietary consumption of trans fatty acids decreases brain docosahexaenoic acid but does not alter amyloid-β and tau pathologies in the 3xTg-AD model of Alzheimer's disease. Neuroscience 2009; 159: 296-307.

[8] Chavarro JE, Rich-Edwards JW, Rosner BA, Willett WC. Dietary fatty acid intakes and the risk of ovulatory infertility. Am J Clin Nutr 2007; 85: 231-7.

[9] Brouwer IA, Wanders AJ, Katan MB. Effect of animal and industrial trans fatty acids on HDL and LDL cholesterol levels in humans-a quantitative review. PloS one 2010; 5: e9434.

[10] Nagaya T, Tanaka N, Komatsu M, Ichijo T, Sano K, Horiuchi A, et al. Development from simple steatosis to liver cirrhosis and hepatocellular carcinoma: a 27-year follow-up case. Clin J Gastroenterol 2008; 1: 116-21.

[11] Nagaya T, Tanaka N, Suzuki T, Sano K, Horiuchi A, Komatsu M, et al. Down-regulation of SREBP-1c is associated with the development of burned-out NASH. J Hepatol 2010; 53: 724-31.

[12] Cohen JC, Horton JD, Hobbs HH. Human fatty liver disease: old questions and new insights. Science 2011; 332: 1519-23.

[13] Yamamoto M, Takeda K. Current views of toll-like receptor signaling pathways. Gastroenterol Res Pract 2010; 2010:240365.

[14] Szabo G, Velayudham A, Romics L, Mandrekar P. Modulation of non-alcoholic steatohepatitis by pattern recognition receptors in mice: the role of toll-like receptors 2 and 4. Alcohol Clin Exp Res 2005; 29 (s2):140S–145S.

[15] Nagoshi S. Osteopontin: Versatile modulator of liver diseases. Hepatol Res 2014; 44: 22-30.

[16] Obara N, Fukushima K, Ueno Y, Wakui Y, Kimura O, Tamai K, et al. Possible involvement and the mechanisms of excess trans-fatty acid consumption in severe NAFLD in mice. J Hepatol 2010; 53: 326-34.

[17] Machado RM, Stefano JT, Oliveira CP, Mello ES, Ferreira FD, Nunes VS, et al. Intake of trans fatty acids causes nonalcoholic steatohepatitis and reduces adipose tissue fat content. J Nutr 2010; 140: 1127-32.

[18] Dhibi M, Brahmi F, Mnari A, Houas Z, Chargui I, Bchir L, et al. The intake of high fat diet with different trans fatty acid levels differentially induces oxidative stress and nonalcoholic fatty liver disease (NAFLD) in rats. Nutr Metab (Lond) 2011; 8: 65.

[19] Okada Y, Tsuzuki Y, Ueda T, Hozumi H, Sato S, Hokari R, et al. Trans fatty acids in diets act as a precipitating factor for gut inflammation? J Gastroenterol Hepatol 2013; 28: 29-32.

[20] Nakajima T, Kamijo Y, Tanaka N, Sugiyama E, Tanaka E, Kiyosawa K, et al. Peroxisome proliferator-activated receptor α protects against alcohol-induced liver damage. Hepatology 2004; 40: 972-80.

[21] Tanaka N, Moriya K, Kiyosawa K, Koike K, Gonzalez FJ, Aoyama T. PPARα activation is essential for HCV core protein-induced hepatic steatosis and hepatocellular carcinoma in mice. J Clin Invest 2008; 118: 683-94.

[22] Komatsu M, Kimura T, Yazaki M, Tanaka N, Yang Y, Nakajima T, et al. Steatogenesis in adult-onset type II citrullinemia is associated with down-regulation of PPARα. Biochim Biophys Acta 2015; 1852: 473-81.

[23] Okiyama W, Tanaka N, Nakajima T, Tanaka E, Kiyosawa K, Gonzalez FJ, et al. Polyenephosphatidylcholine prevents alcoholic liver disease in PPARα-null mice through attenuation of increases in oxidative stress. J Hepatol 2009; 50: 1236-46.

[24] Tanaka N, Matsubara T, Krausz KW, Patterson AD, Gonzalez FJ. Disruption of phospholipid and bile acid homeostasis in mice with nonalcoholic steatohepatitis. Hepatology 2012; 56: 118-29.

[25] Tanaka N, Takahashi S, Fang ZZ, Matsubara T, Krausz KW, Qu A, et al. Role of white adipose lipolysis in the development of NASH induced by methionine-and choline-deficient diet. Biochim Biophys Acta 2014; 1841: 1596-607.

[26] Tanaka N, Takahashi S, Matsubara T, Jiang C, Sakamoto W, Chanturiya T, et al. Adipocyte-specific disruption of fat-specific protein 27 causes hepatosteatosis and insulin resistance in high-fat diet-fed mice. J Biol Chem 2015; 290: 3092-105.

[27] Tanaka N, Takahashi S, Zhang Y, Krausz KW, Smith PB, Patterson AD, et al. Role of fibroblast growth factor 21 in the early stage of NASH induced by methionine-and choline-deficient diet. Biochim Biophys Acta 2015; 1852: 1242-52.

[28] Aoyama T, Yamano S, Waxman DJ, Lapenson DP, Meyer UA, Fischer V, et al. Cytochrome P-450 hPCN3, a novel cytochrome P-450 IIIA gene product that is differentially expressed in adult human liver. cDNA and deduced amino acid sequence and distinct specificities of cDNA-expressed hPCN1 and hPCN3 for the metabolism of steroid hormones and cyclosporine. J Biol Chem 1989; 264: 10388-395.

[29] Aoyama T, Peters JM, Iritani N, Nakajima T, Furihata K, Hashimoto T, et al. Altered constitutive expression of fatty acid-metabolizing enzymes in mice lacking the peroxisome proliferator-activated receptor α (PPARα). J Biol Chem 1998; 273: 5678-84.

[30] Pahl HL. Activators and target genes of Rel/NF-κB transcription factors. Oncogene 1999; 18: 6853-66.

[31] Bhardwaj S, Passi SJ, Misra A. Overview of trans fatty acids: biochemistry and health effects. Diabetes Metab Syndr 2011; 5: 161-4.

[32] Cassagno N, Palos-Pinto A, Costet P, Breilh D, Darmon M, Bérard AM. Low amounts of trans 18: 1 fatty acids elevate plasma triacylglycerols but not cholesterol and alter the cellular defence to oxidative stress in mice. Br J Nutr 2005; 94: 346-52.

[33] Mitmesser SH, Carr TP. Trans fatty acids alter the lipid composition and size of apoB-100-containing lipoproteins secreted by HepG2 cells. J Nutr Biochem 2005; 16: 178-83.

[34] Estadella D, da Penha Oller do Nascimento CM, Oyama LM, Ribeiro EB, Dâmaso AR, de Piano A. Lipotoxicity: effects of dietary saturated and trans fatty acids. Mediators Inflamm 2013; 2013:137579.

[35] Tak PP, Firestein GS. NF-κB: a key role in inflammatory diseases. J Clin Invest 2001; 107: 7-11.

[36] Wullaert A, Heyninck K, Beyaert R. Mechanisms of crosstalk between TNF-induced NF-κB and JNK activation in hepatocytes. Biochem Pharmacol 2006; 72: 1090-101.

[37] Nagaya T, Tanaka N, Kimura T, Kitabatake H, Fujimori N, Komatsu M, et al. Mechanism of the development of nonalcoholic steatohepatitis after pancreaticoduodenectomy. BBA Clin 2015; 3: 168-74.

[38] Miura K, Seki E, Ohnishi H, Brenner DA. Role of toll-like receptors and their downstream molecules in the development of nonalcoholic fatty liver disease. Gastroenterol Res Pract 2010; 2010:362847.

[39] Sahai A, Malladi P, Melin-Aldana H, Green RM, Whitington PF. Upregulation of osteopontin expression is involved in the development of nonalcoholic steatohepatitis in a dietary murine model. Am J Physiol Gastrointest Liver Physiol 2004; 287: G264-73.

[40] Lee SH, Seo GS, Park YN, Yoo TM, Sohn DH. Effects and regulation of osteopontin in rat hepatic stellate cells. Biochem Pharmacol 2004; 68: 2367-78.

[41] Salvi V, Scutera S, Rossi S, Zucca M, Alessandria M, Greco D, et al. Dual regulation of osteopontin production by TLR stimulation in dendritic cells. J Leukoc Biol 2013; 94: 147-58.

[42] Strowig T, Henao-Mejia J, Elinav E, Flavell R. Inflammasomes in health and disease. Nature 2012; 481: 278-86.

[43] Szabo G, Csak T. Inflammasomes in liver diseases. J Hepatol 2012; 57: 642-54.

[44] Csak T, Ganz M, Pespisa J, Kodys K, Dolganiuc A, Szabo G. Fatty acid and endotoxin activate inflammasomes in mouse hepatocytes that release danger signals to stimulate immune cells. Hepatology 2011; 54: 133-44.

[45] Tailleux A, Wouters K, Staels B. Roles of PPARs in NAFLD: potential therapeutic targets. Biochim Biophys Acta 2012; 1821: 809-18.

Figure Legends

Figure 1. Anthropometric and biochemical parameters and histological findings of the liver.

Male 10- to 14-week-old Sv/129 wild-type (WT) and *Ppara*-null (KO) mice were treated with AIN93G diet (CON) or one replacing most of FA to *trans*-FA (TFA) for two months.

(**A**) Body weight and weight of epididymal fat pad (EFP) and liver.

(**B**) Serum levels of alanine aminotransferase (ALT) and triglyceride (TG) and hepatic TG contents.

(**C**) Representative photomicrographs of hematoxylin and eosin-stained liver sections. Upper and lower rows show a lower (x20) and higher (x100) magnification, respectively. Hepatocytes of TFA diet-treated KO mice showed abundant large lipid droplets and infiltration of inflammatory cells (arrow).

Results are expressed as mean ± SEM. $^{*}P<0.05$, $^{***}P<0.001$ between TFA diet-treated WT and KO mice: $^{\#\#}P<0.01$, $^{\#\#\#}P<0.001$ vs. control diet in the same genotype.

Figure 2. Hepatic expression of genes associated with FA synthesis and uptake in the liver.

(**A**) Hepatic mRNA levels of genes related to fatty acid (FA) *de novo* synthesis (*Fasn* and *Acaca*) and FA uptake (*Cd36*) were quantified by qPCR, normalized to those of *Gapdh* mRNA levels, and expressed as values relative to wild-type (WT) mice fed a control diet. Results are expressed as mean ± SEM. KO, *Ppara*-null mice: $^{**}P<0.01$, $^{***}P<0.001$, between TFA diet-treated WT and KO mice: $^{\#}P<0.05$, $^{\#\#}P<0.01$ vs. control diet in the same genotype.

(**B and C**) Immunoblot analysis of FA-synthesizing enzymes (FAS and ACCα) and FA transporter (CD36). Whole liver homogenates (20-40 μg of proteins) were loaded in each well and the band of β-actin was used as a loading control. The band intensity was measured densitometrically, normalized to those of β-actin, and expressed as values relative to WT mice fed a control diet. Results were obtained from two independent immunoblot experiments and expressed as mean ± SEM. $^{*}P<0.05$

between TFA diet-treated WT and KO mice: $^{\#}P<0.05$, $^{\#\#}P<0.01$ vs. control diet in the same genotype.

Figure 3. Reduced FA utilization in TFA-containing diet-treated *Ppara-null* (KO) mice compared with similarly-treated wild-type (WT) mice.

(**A**) Hepatic mRNA levels of genes related to intracellular fatty acid (FA) carriage (*Fabp1*) and FA activation (*Acsl1*) and catabolism (*Acadl* and *Acadvl*) were quantified by qPCR, normalized to those of *Gapdh* mRNA levels, and expressed as values relative to WT mice fed a control diet. Results are expressed as mean ± SEM. $^{**}P<0.01$, $^{***}P<0.001$ between TFA diet-treated WT and KO mice.

(**B and C**) Immunoblot analysis of the corresponding proteins involved in intracellular FA carriage (FABP1) and FA activation (LACS) and catabolism (LCAD and VLCAD). Whole liver homogenates (20-60 μg of proteins) were loaded in each well and the band of β-actin was used as a loading control. The band intensity was measured densitometrically, normalized to those of β-actin, and expressed as values relative to WT mice fed a control diet. Results were obtained from two independent immunoblot experiments and expressed as mean ± SEM. $^{*}P<0.05$, $^{**}P<0.01$, $^{***}P<0.001$ between TFA diet-treated WT and KO mice.

Figure 4. Hepatic mRNA levels of genes associated with TG turnover in the liver.

(**A**) Hepatic mRNA levels of genes related to triglyceride (TG) synthesis (*Dgat1* and *Dgat2*), excretion to the circulation (*Mttp*), and hydrolysis (*Pnpla2 and Lipe*) were quantified by qPCR, normalized to those of *Gapdh* mRNA levels, and expressed as values relative to wild-type (WT) mice fed a control diet. Results are expressed as mean ± SEM. KO, *Ppara*-null mice: $^{\#}P<0.05$, $^{\#\#}P<0.01$ vs. control diet in the same genotype.

(**B and C**) Immunoblot analysis of microsomal TG transfer protein (MTP) and adipose TG lipase (ATGL). Whole liver homogenates (20-30 μg of proteins) were loaded in each well and the band of β-actin was used as a loading control. The band intensity was measured densitometrically, normalized to those of β-actin, and

expressed as values relative to WT mice fed a control diet. Results were obtained from two independent immunoblot experiments and expressed as mean ± SEM. $^{\#\#}P<0.01$, $^{\#\#\#}P<0.001$ vs. control diet in the same genotype.

Figure 5. Aggravated hepatic inflammation in TFA-containing diet-treated *Ppara-null* (KO) mice compared with similarly-treated wild-type (WT) mice.

(**A**) Hepatic mRNA levels of pro-inflammatory mediators, *Tnf* (encoding tumor necrosis factor α), *Ccl2* (monocyte chemoattractant protein 1), *Spp1* (osteopontin, OPN), and *Col1a1* (collagen 1a1) were measured by qPCR, normalized to those of *Gapdh* mRNA levels, and subsequently expressed as values relative to WT mice fed a control diet. Results are expressed as mean ± SEM. $^{*}P<0.05$ between TFA diet-treated WT and KO mice.

(**B and C**) Immunoblot analysis of OPN and NF-κB p65. Whole liver homogenates (20-40 μg of proteins, W) and liver nuclear fractions (30 μg of proteins, N) were loaded into each well and the band of β-actin and histone H1 was used as the respective loading control. The band intensity was measured densitometrically, normalized to those of loading control, and expressed as values relative to WT mice fed a control diet. Results were obtained from two independent immunoblot experiments and expressed as mean ± SEM. $^{*}P<0.05$, $^{***}P<0.001$ between TFA diet-treated WT and KO mice: $^{\#\#\#}P<0.001$ vs. control diet in the same genotype.

Figure 6. Hepatic mRNA levels of inflammasome-related genes.

The same samples used in Fig. 2-5 were subjected to qPCR. Results were expressed as mean ± SEM. WT, wild-type mice: KO, *Ppara*-null mice.

Figure 7. Augmented TLR2 expression in TFA-containing diet-treated *Ppara-null* (KO) mice compared with similarly-treated wild-type (WT) mice.

(**A**) Hepatic mRNA levels of genes involved in TLR-mediated signaling were measured by qPCR, normalized to those of *Gapdh* mRNA levels, and subsequently

expressed as values relative to WT mice fed a control diet. Results are expressed as mean ± SEM. $^{*}P<0.05$ between TFA diet-treated WT and KO mice.

(**B and C**) Immunoblot analysis of TLR2. Whole liver homogenates (20-50 μg of proteins) were loaded into each well and the band of β-actin was used as a loading control. The band intensity was measured densitometrically, normalized to those of β-actin, and expressed as values relative to WT mice fed a control diet. Results were obtained from two independent immunoblot experiments and expressed as mean ± SEM. $^{***}P<0.001$ between TFA diet-treated WT and KO mice: $^{\#}P<0.05$ vs. control diet in the same genotype.

Figure 1

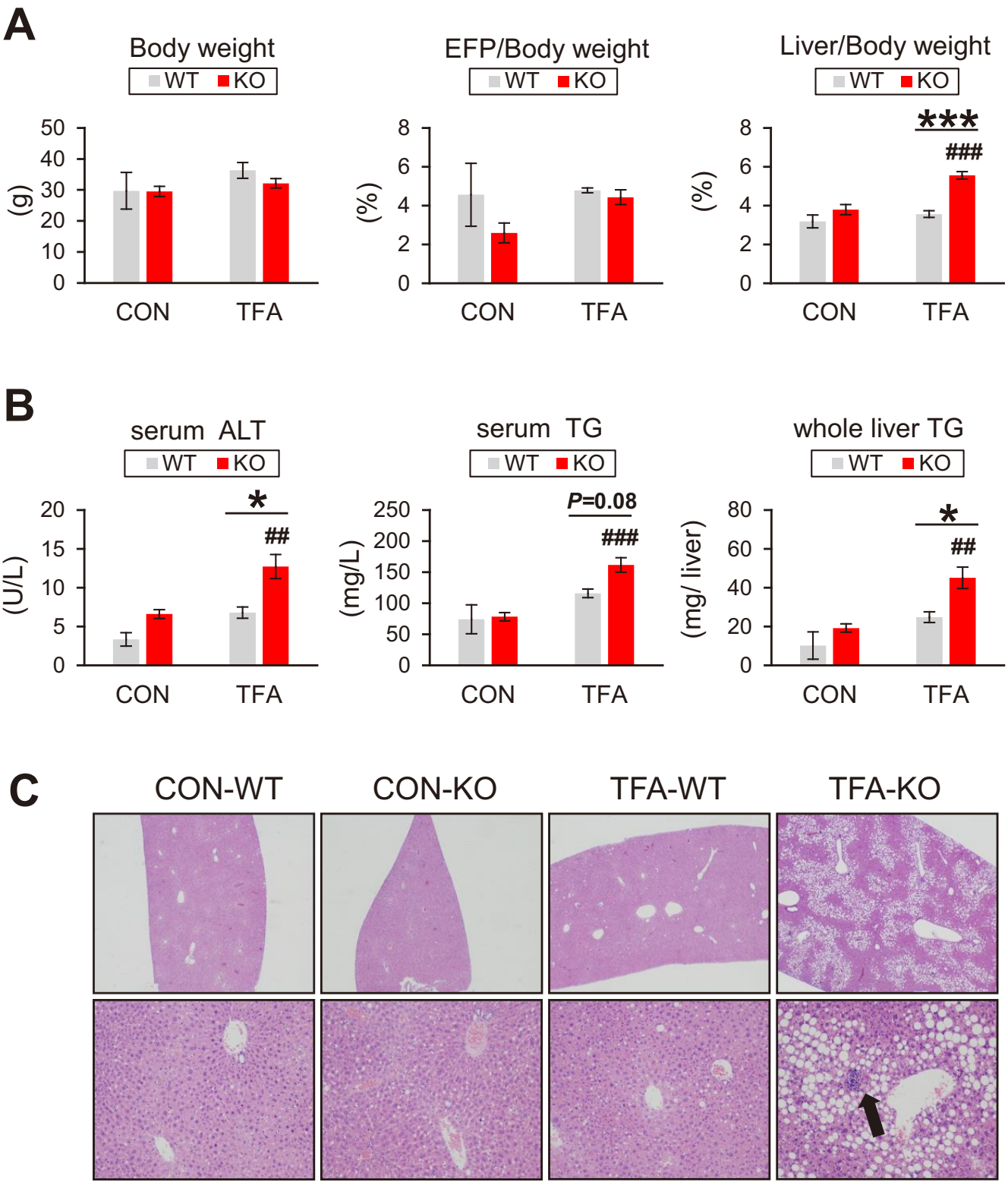
A
Body weight
WT KO
(g)
50
40
30
20
10
0
CON
TFA
EFP/Body weight
WT KO
(%)
8
6
4
2
0
CON
TFA
Liver/Body weight
WT KO
***
###
(%)
8
6
4
2
0
CON
TFA
B
serum ALT
WT KO
*
##
(U/L)
20
15
10
5
0
CON
TFA
serum TG
WT KO
P=0.08
###
(mg/L)
250
200
150
100
50
0
CON
TFA
whole liver TG
WT KO
*
##
(mg/ liver)
80
60
40
20
0
CON
TFA
C
CON-WT
CON-KO
TFA-WT
TFA-KO

Figure 2

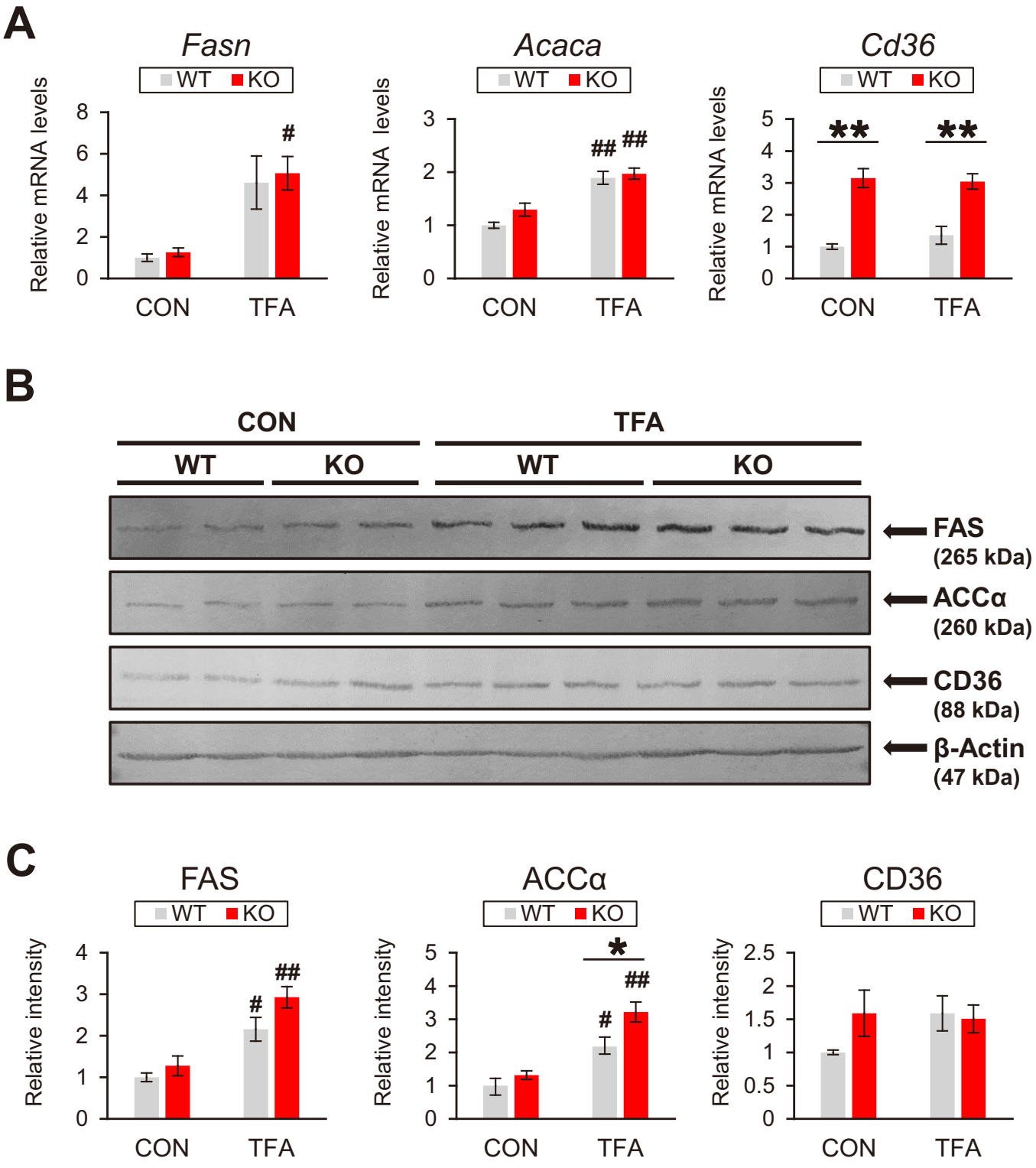
A
Fasn
Acaca
Cd36
WT
KO
Relative mRNA levels
CON
TFA
#
##
**
B
CON
TFA
WT
KO
FAS
(265 kDa)
ACCα
(260 kDa)
CD36
(88 kDa)
β-Actin
(47 kDa)
C
FAS
ACCα
CD36
Relative intensity
*

Figure 3

A

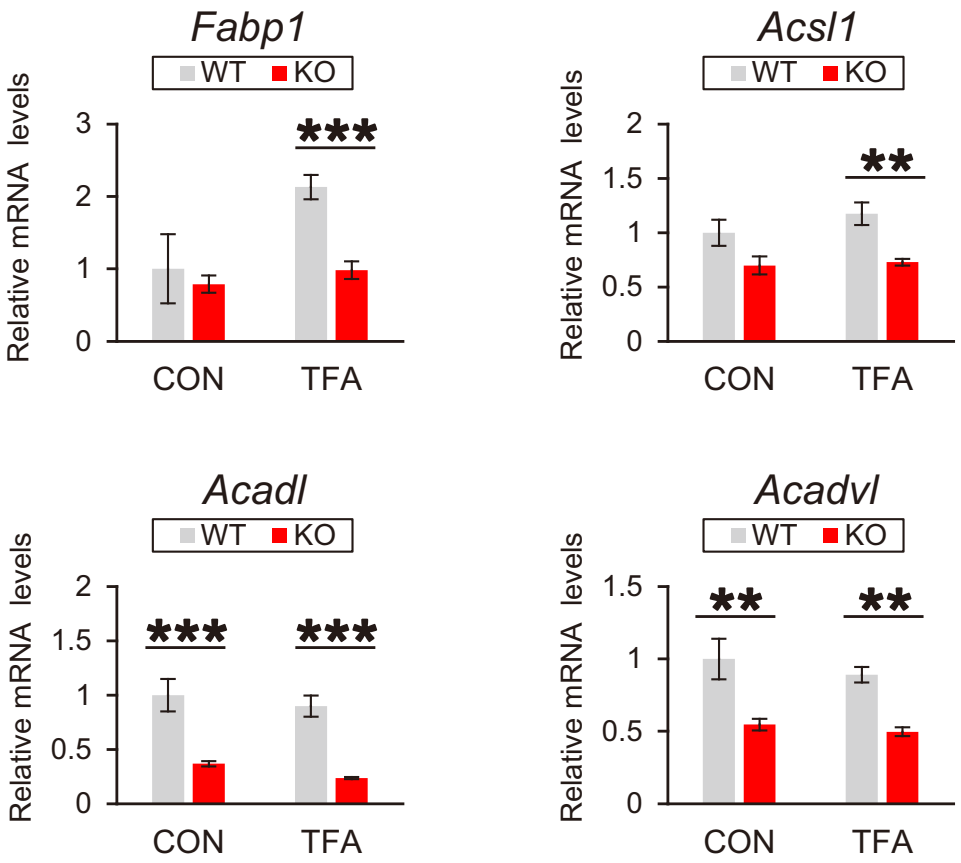
Fabp1
WT
KO
Relative mRNA levels
3
2
1
0
***
CON
TFA
Acsl1
WT
KO
Relative mRNA levels
2
1.5
1
0.5
0
**
CON
TFA
Acadl
WT
KO
Relative mRNA levels
2
1.5
1
0.5
0
***
***
CON
TFA
Acadvl
WT
KO
Relative mRNA levels
1.5
1
0.5
0
**
**
CON
TFA

Figure 3

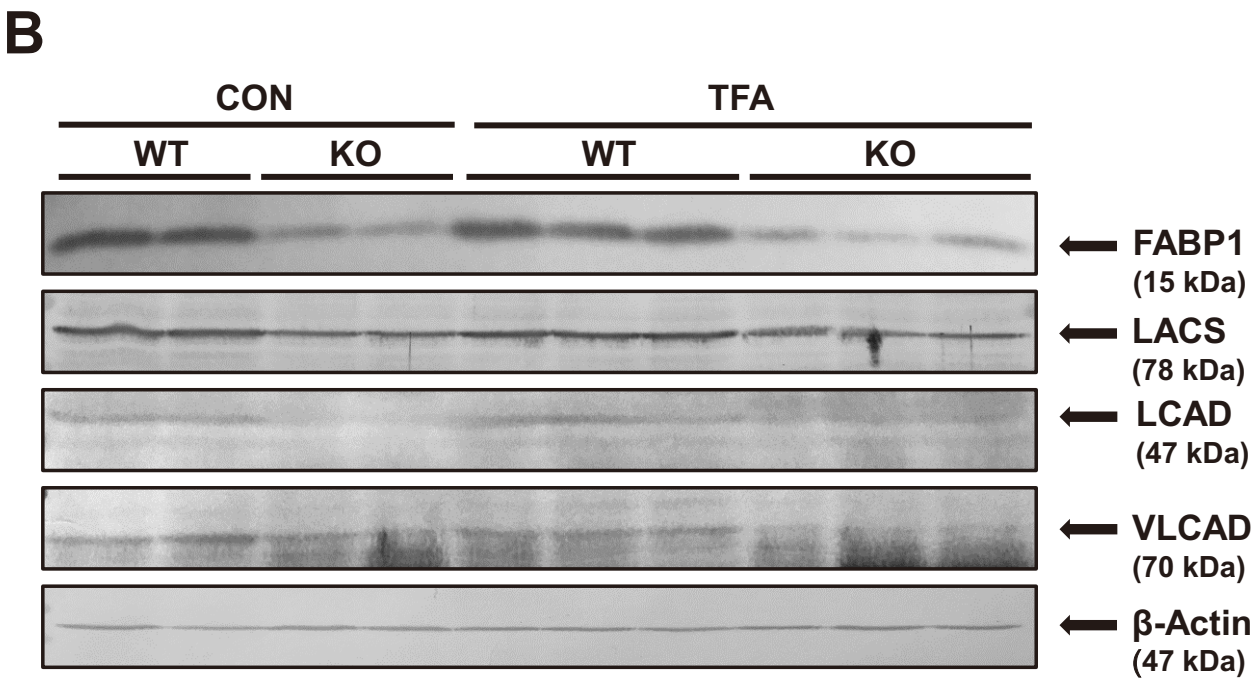
B
CON
TFA
WT
KO
WT
KO
FABP1
(15 kDa)
LACS
(78 kDa)
LCAD
(47 kDa)
VLCAD
(70 kDa)
β-Actin
(47 kDa)

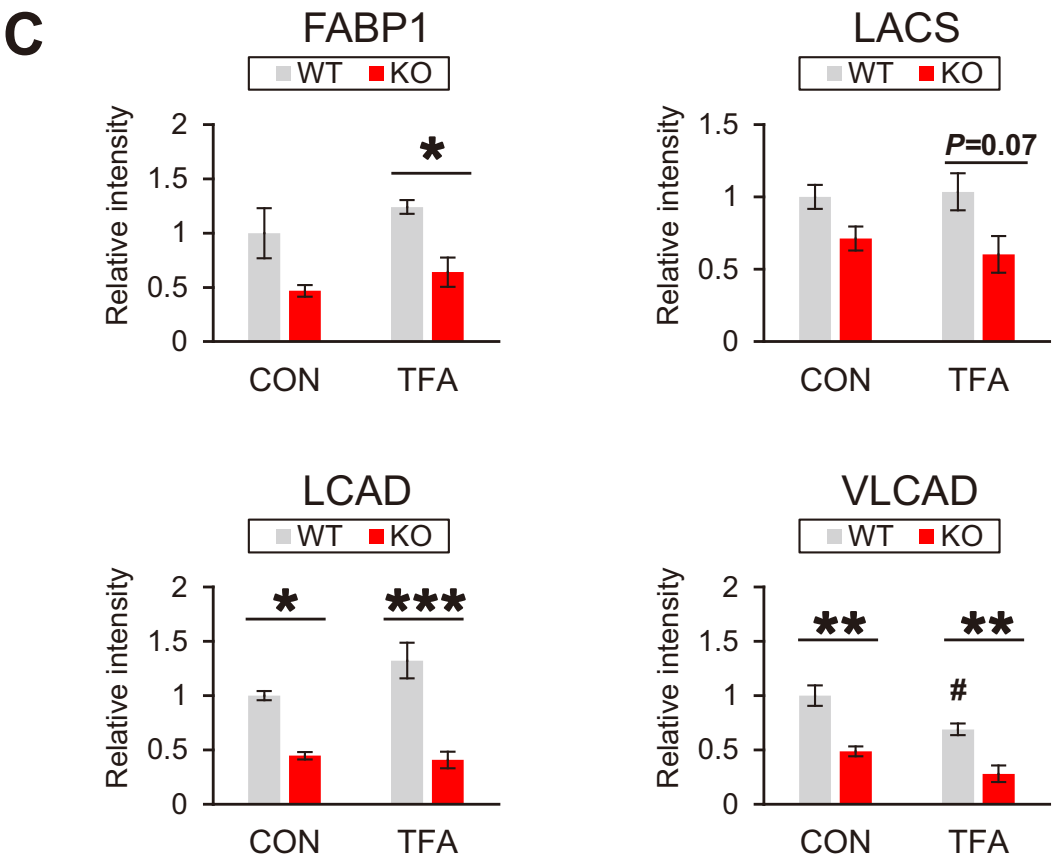
C
FABP1
WT KO
Relative intensity
2
1.5
1
0.5
0
*
CON
TFA
LACS
WT KO
Relative intensity
1.5
1
0.5
0
P=0.07
CON
TFA
LCAD
WT KO
Relative intensity
2
1.5
1
0.5
0
*
***
CON
TFA
VLCAD
WT KO
Relative intensity
2
1.5
1
0.5
0
**
**
#
CON
TFA

Figure 4

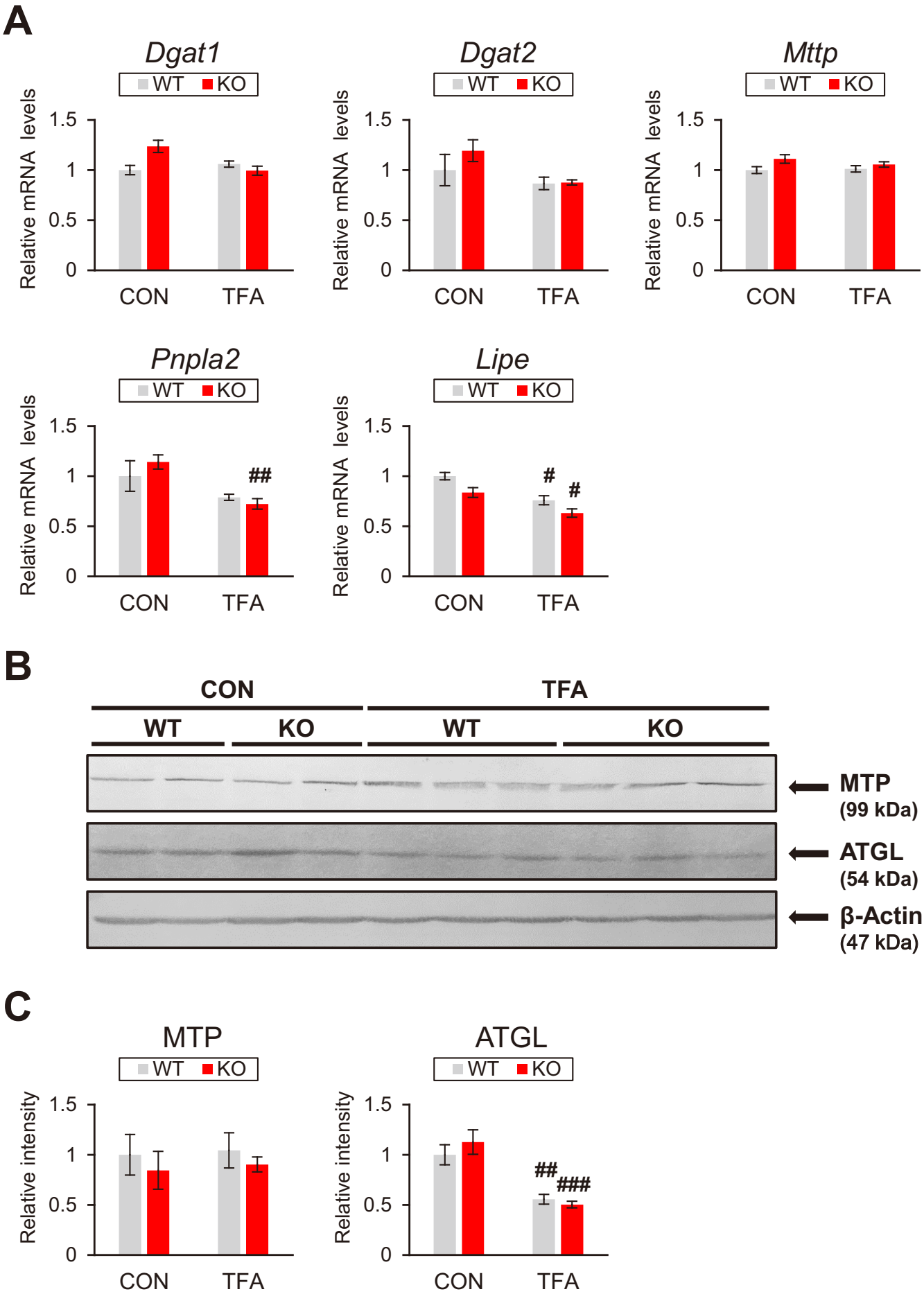
A
Dgat1
Dgat2
Mttp
Pnpla2
Lipe
WT
KO
Relative mRNA levels
1.5
1
0.5
0
CON
TFA
##
#
B
CON
TFA
WT
KO
MTP
(99 kDa)
ATGL
(54 kDa)
β-Actin
(47 kDa)
C
MTP
ATGL
Relative intensity
###

Figure 5

A

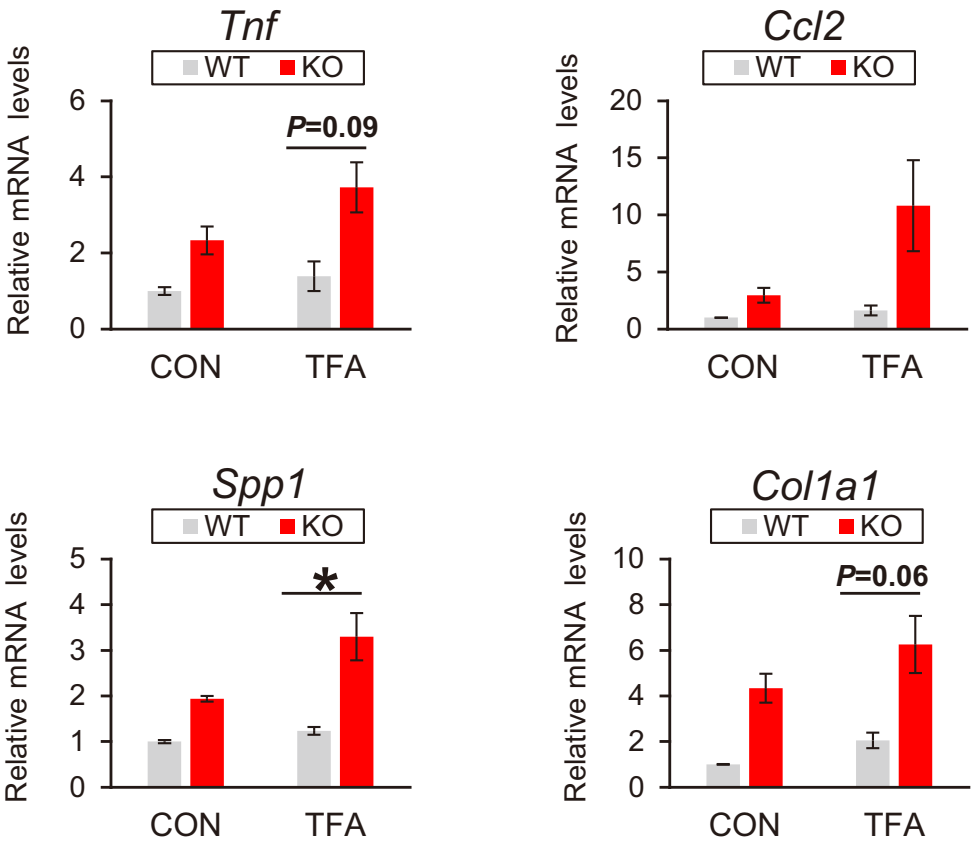
Tnf
WT
KO
P=0.09
Relative mRNA levels
6
4
2
0
CON
TFA
Ccl2
WT
KO
Relative mRNA levels
20
15
10
5
0
CON
TFA
Spp1
WT
KO
*
Relative mRNA levels
5
4
3
2
1
0
CON
TFA
Col1a1
WT
KO
P=0.06
Relative mRNA levels
10
8
6
4
2
0
CON
TFA

Figure 5

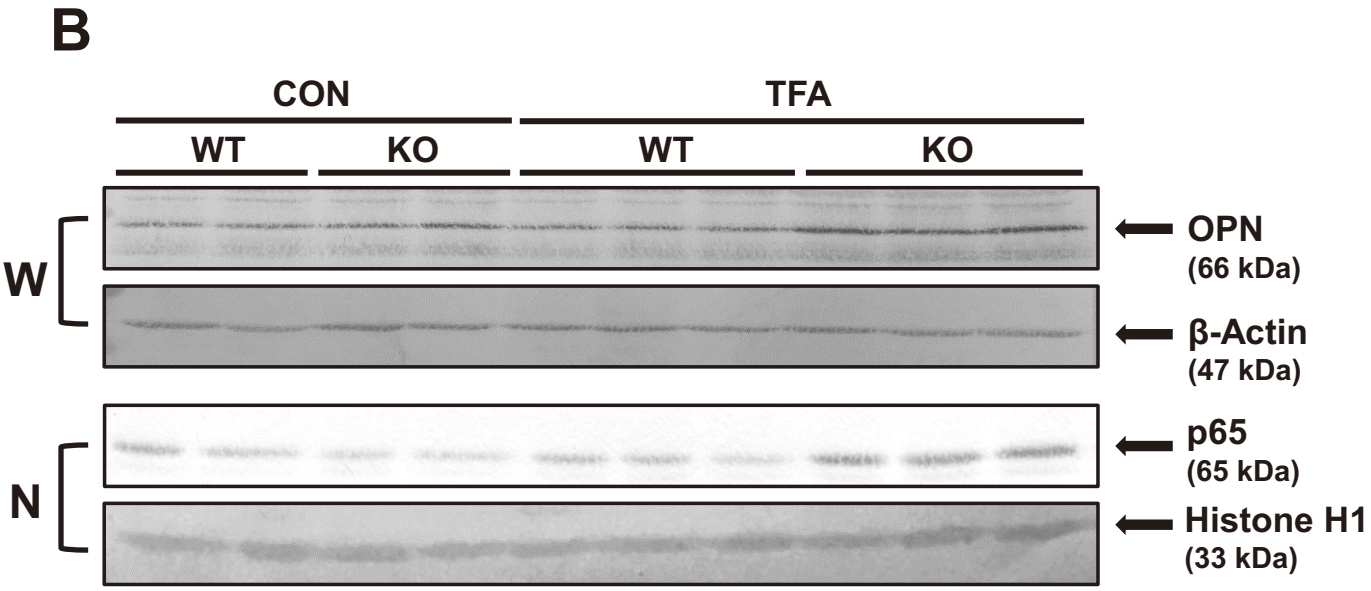
B
CON
TFA
WT
KO
WT
KO
W
N
OPN
(66 kDa)
β-Actin
(47 kDa)
p65
(65 kDa)
Histone H1
(33 kDa)

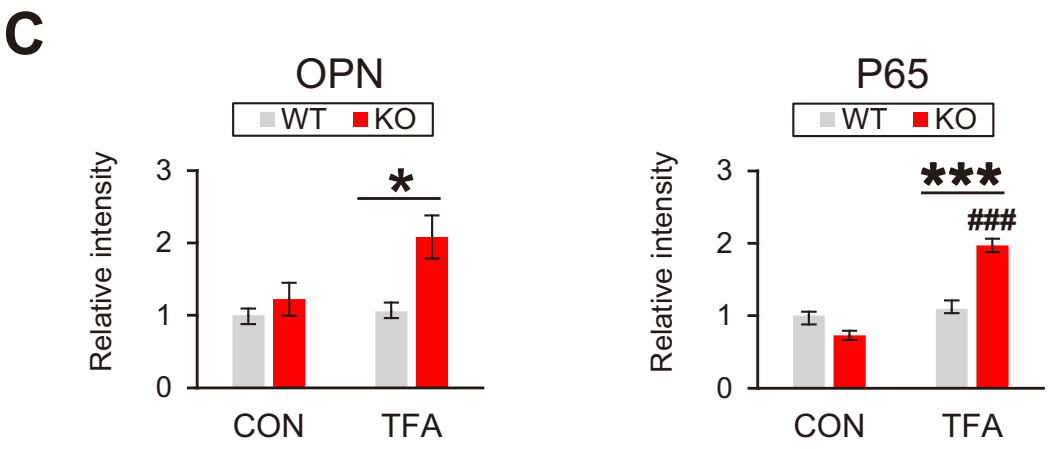
C
OPN
WT
KO
Relative intensity
3
2
1
0
*
CON
TFA
P65
WT
KO
Relative intensity
3
2
1
0
***
###
CON
TFA

Figure 6

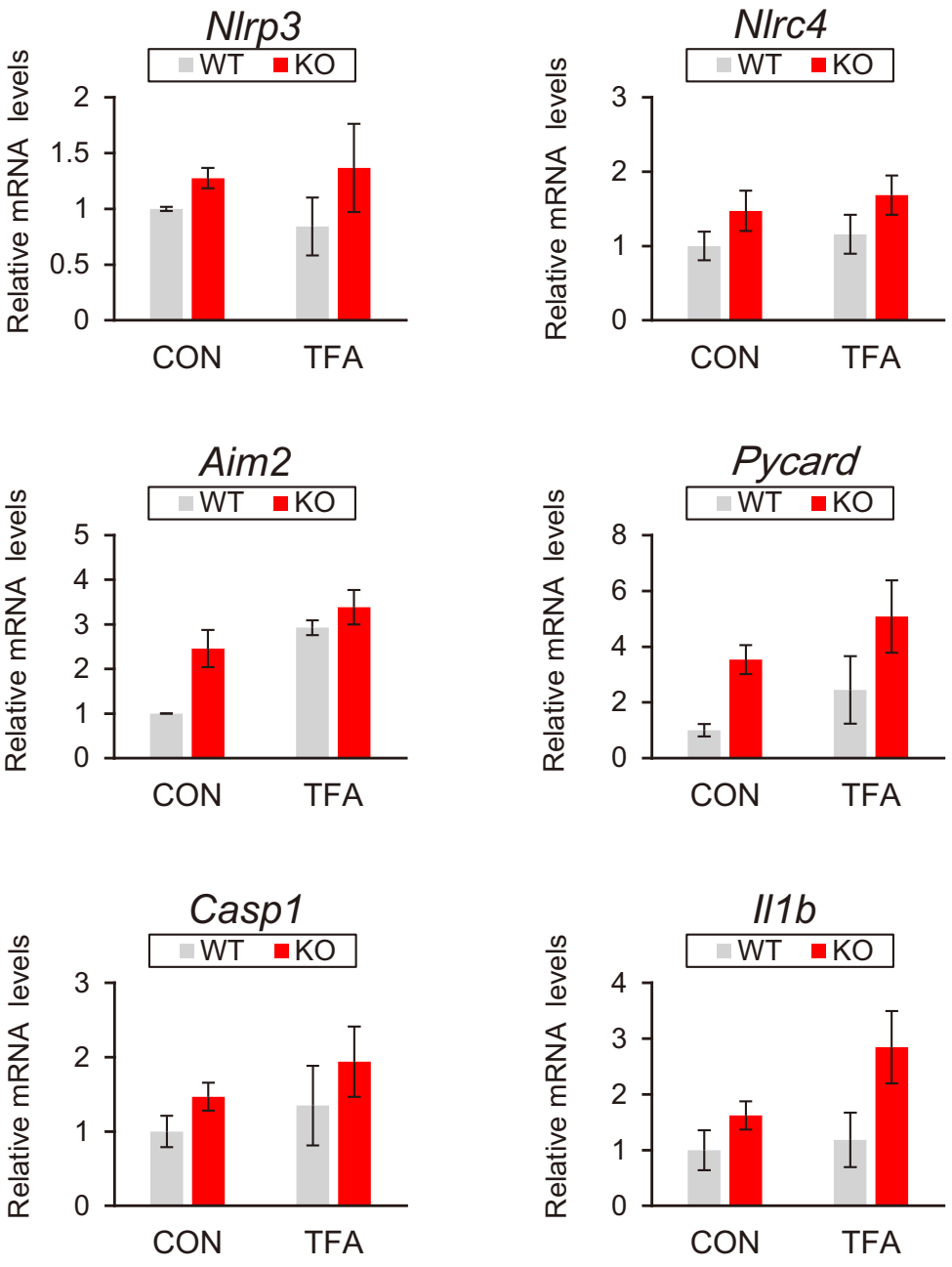
Nlrp3
WT KO
Relative mRNA levels
2
1.5
1
0.5
0
CON
TFA
Nlrc4
WT KO
Relative mRNA levels
3
2
1
0
CON
TFA
Aim2
WT KO
Relative mRNA levels
5
4
3
2
1
0
CON
TFA
Pycard
WT KO
Relative mRNA levels
8
6
4
2
0
CON
TFA
Casp1
WT KO
Relative mRNA levels
3
2
1
0
CON
TFA
Il1b
WT KO
Relative mRNA levels
4
3
2
1
0
CON
TFA

Figure 7

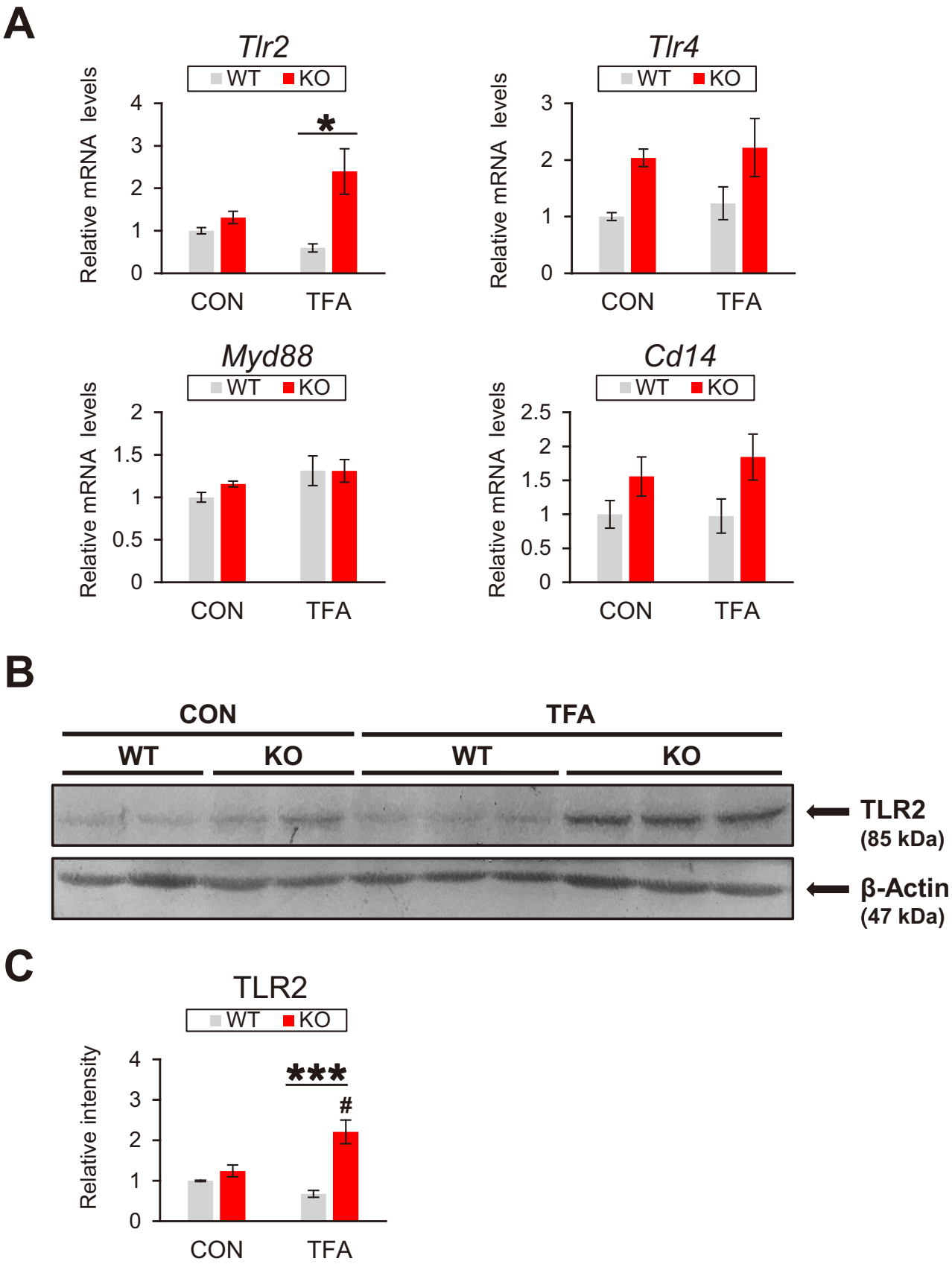
A
Tlr2
WT KO
Relative mRNA levels
4
3
2
1
0
*
CON
TFA
Tlr4
WT KO
Relative mRNA levels
3
2
1
0
CON
TFA
Myd88
WT KO
Relative mRNA levels
2
1.5
1
0.5
0
CON
TFA
Cd14
WT KO
Relative mRNA levels
2.5
2
1.5
1
0.5
0
CON
TFA
B
CON
TFA
WT
KO
WT
KO
TLR2
(85 kDa)
β-Actin
(47 kDa)
C
TLR2
WT KO
Relative intensity
4
3
2
1
0
***
#
CON
TFA

Supporting information

PPARα protects against *trans*-fatty acid-containing diet-induced steatohepatitis

Hu Xiao[1], Naoki Tanaka[1], Guo Ran[1], Lu Yu[1], Takero Nakajima[1], Frank J. Gonzalez[2], and Toshifumi Aoyama[1]

[1]Department of Metabolic Regulation, Shinshu University Graduate School of Medicine, Matsumoto, Japan

[2]Laboratory of Metabolism, Center for Cancer Research, National Cancer Institute, National Institutes of Health, Bethesda, MD

Correspondence: Naoki Tanaka, M.D., Ph. D. Department of Metabolic Regulation, Shinshu University Graduate School of Medicine, 390-8621, Matsumoto, Japan
e-mail: naopi@shinshu-u.ac.jp; Tel: +81-263-37-2851

Supplementary Figure 1. Hepatic mRNA levels of genes associated with oxidative stress and ER stress oxygen species-generating/eliminating and ER stress-inducible transcription factor.

Hepatic mRNA levels of genes encoding reactive oxygen species-generating/eliminating enzymes (**A** and **B**) and ER stress-inducible transcription factor (**C**) were quantified by qPCR, normalized to those of *Gapdh* mRNA levels, and expressed as values relative to wild-type (WT) mice fed a control diet. Results are expressed as mean ± SEM. KO, *Ppara*-null mice: **P*<0.05, ***P*<0.01 between WT and KO mice in the same diet.

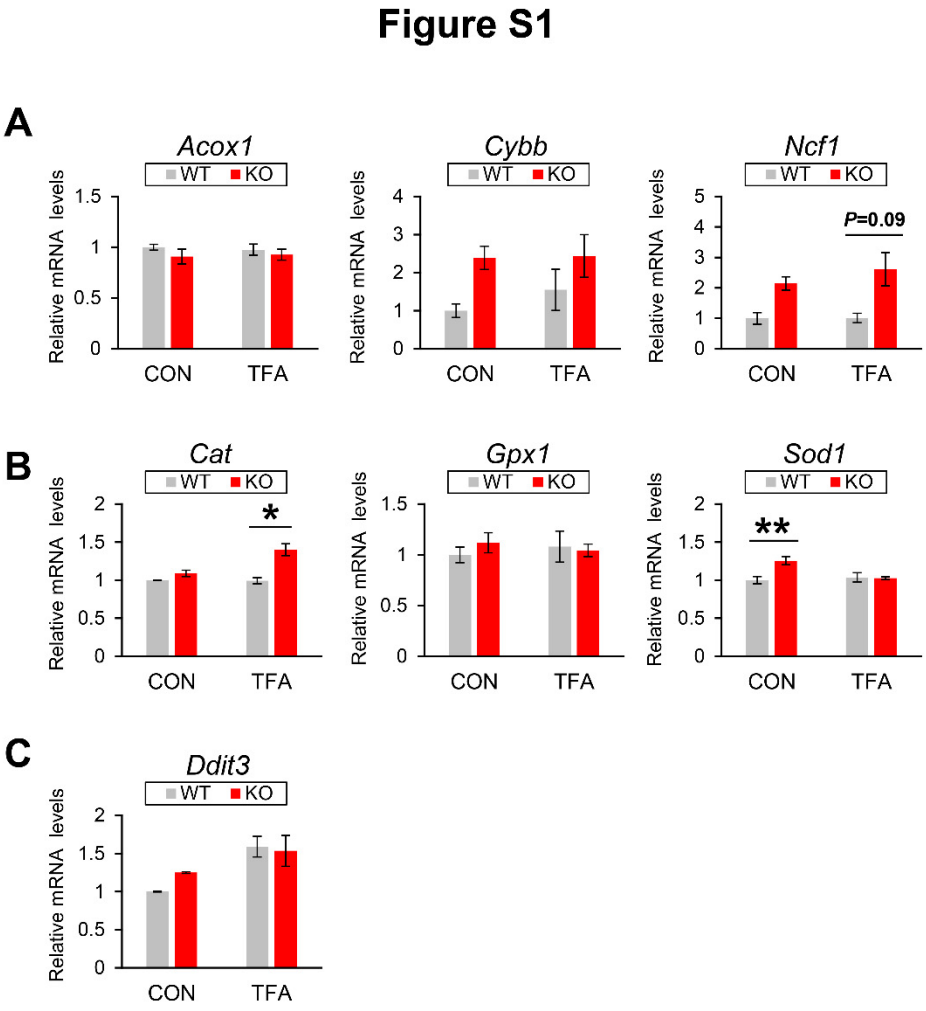

Supplementary Table 1. Nutrient composition of control AIN93G and TFA-containing AIN93G diets

	CON diet	TFA diet
Protein	20	20
Carbohydrate	64	64
Fat	7	7
kcal/g	4	4
Casein	200	200
L-Cystine	3	3
Corn Starch	397	397
Maltodextrin	132	132
Sucrose	100	100
Cellulose	50	50
t-Butylhydroquinone	0.014	0.014
Mineral Mix	35	35
Vitamin Mix	10	10
Choline Bitartrate	2.5	2.5
Soybean Oil	70	10
Primex	0	60

Values indicate g/kg of diet.

Supplementary Table 2. Fatty acid composition of control AIN93G and TFA-containing AIN93G diets.

	CON diet	TFA diet
Lauric, C12:0	0	0.06
Myristic, C14:0	0	0.13
Palmitic, C16:0	7.28	10.9
Palmitoleic, C16:1	0	0.07
Stearic, C18:0	2.66	7.29
Elaidic, C18:1 *trans*	0	13.7
Oleic, C18:1 *cis*	17.0	24.6
Linoelaidic, C18:2 *trans*	0	1.86
Linoleic, C18:2 *cis*	37.4	9.32
Linoelaidic, C18:3 *trans*	0	0.12
Linolenic, C18:3 *cis*	5.46	0.92
Arachidic, C20:0	0	0.22
Eicosenoic, C20:1	0	0.09
Behenic, C22:0	0	0.21
Lignoceric, C24:0	0	0.08
Total fatty acid (g)	69.9	69.7
Saturated fatty acid (g)	9.9	18.9
Monounsaturated fatty acid (g)	17	24.8
Polyunsaturated fatty acid (g)	42.9	9.5
Trans fatty acid (g)	0	15.7

Values indicate g/kg of diet.

Supplementary Table 3. Primer pairs used for qPCR.

Gene	Genebank Accenssion Number		primer sequence (5'-3')
Acaca	NM_133360	F	GGGCACAGACCGTGGTAGTT
		R	CAGGATCAGCTGGGATACTGAGT
Acadl	NM_007381	F	TTTCCGGGAGAGTGTAAGGA
		R	ACTTCTCCAGCTTTCTCCCA
Acadvl	NM_017366	F	CCGGTTCTTTGAGGAAGTGAA
		R	AGTGTCGTCCTCCACCTTCTC
Acox1	NM_015729	F	TGGTATGGTGTCGTACTTGAATGAC
		R	AATTTCTACCAATCTGGCTGCAC
Acsl	NM_007981	F	TCCTACGGCAGTGATCTGGTG
		R	GGTTGCCTGTAGTTCCACTTGTG
Aim2	NM_001013779	F	GGAACAATTGTGAATGGGCT
		R	TTGTCTCCTTCCTCGCACTT
Cat	NM_009804	F	CGACCAGGGCATCAAAAACTT
		R	AACGTCCAGGACGGGTAATTG
Casp1	NM_009807	F	TACCTGGCAGGAATTCTGGA
		R	AGTCCTGGAAATGTGCCATC
Ccl2	NM_011333	F	AGGTCCCTGTCATGCTTCTG
		R	GGGATCATCTTGCTGGTGAA
Cd14	NM_009841	F	CTCTGTCCTTAAAGCGGCTTAC
		R	GTTGCGGAGGTTCAAGATGTT
Cd36	NM_007643	F	CCAAATGAAGATGAGCATAGGACAT
		R	GTTGACCTGCAGTCGTTTTGC
Col1a1	NM_007742	F	ACATGTTCAGCTTTGTGGACC
		R	TAGGCCATTGTGTATGCAGC
Cybb	NM_007807	F	GAAAACTCCTTGGGTCAGCACT
		R	ATTTCGACACACTGGCAGCA
Ddit3	NM_007837	F	CAGCGACAGAGCCAGAATAA
		R	GACCAGGTTCTGCTTTCAGG
Dgat1	NM_010046	F	CTGCTACGACGAGTTCTTGAGA
		R	GATAGTAGGGACCATCCACTGTTG
Dgat2	NM_026384	F	GCTTCGCGAGTACCTGATGT
		R	CACCACGATGATGATAGCATTG
Fabp1	NM_017399	F	GCAGAGCCAGGAGAACTTTGAG
		R	TTTGATTTTCTTCCCTTCATGCA
Fasn	NM_007988	F	ATCCTGGAACGAGAACACGATCT
		R	AGAGACGTGTCACTCCTGGACTT
Gpx1	NM_008160	F	CCAGGAGAATGGCAAGAATGA
		R	TCTCACCATTCACTTCGCACTT'
ll1b	NM_008361	F	TGAAGCAGCTATGGCAACTG
		R	AGGTCAAAGGTTTGGAAGCA

Lipe	NM_010719	F	GAGCGCTGGAGGAGTGTTTT
		R	TGATGCAGAGATTCCCACCTG
Mttp	NM_008642	F	GAGCGGTCTGGATTTACAACG
		R	GTAGGTAGTGACAGATGTGGCTTTTG
Myd88	NM_010851	F	TCATGTTCTCCATACCCTTGGT
		R	AAACTGCGAGTGGGGTCAG
Ncf1	NM_010876	F	GCCCAAAGATGGCAAGAATAAC
		R	TAGTCAGCAATGGCCCGATAG
Nlrp3	NM_145827	F	GCTCCAACCATTCTCTGACC
		R	AAGTAAGGCCGGAATTCACC
Nlrp4	NM_001033367	F	ATCGTCATCACCGTGTGGAG
		R	GCCAGACTCGCCTTCAATCA
Pnpla2	NM_025802	F	CGTGTTTCAGACGGAGAGAAC
		R	TTGGAGGGTAGGAGGAATGAG
Pycard	NM_023258	F	GAAGCTGCTGACAGTGCAAC
		R	GCCACAGCTCCAGACTCTTC
Sod1	NM_011434	F	AAGCGGTGAACCAGTTGTGTT'
		R	AGCCTTGTGTATTGTCCCCATACT
Spp1	NM_009263	F	CTCCTTGCGCCACAGAATG
		R	TTGGAAGAGTTTCTTGCTTAAAGTCA
Tnf	NM_013693	F	CCACCACGCTCTTCTGTCTAC
		R	AGGGTCTGGGCCATAGAACT
Trl2	NM_011905	F	CATCACCGGTCAGAAAACAA
		R	ACCAAGATCCAGAAGAGCCA
Trl4	NM_021297	F	TGTTCTTCTCCTGCCTGACA
		R	TGTCATCAGGGACTTTGCTG

F, forward sequence; R, reserve sequence.
Acaca, acetyl-coenzyme A carboxylase alpha
Acadl, acyl-coenzyme A dehydrogenase, long-chain
Acadvl, acyl-coenzyme A dehydrogenase, very long chain
Acox1, acyl-coenzyme A oxidase 1, palmitoyl
Acsl, acyl-coA synthetase long-chain
Aim2, absent in melanoma 2
Cat, catalase
Casp1, caspase 1
Ccl2, chemokine (C-C motif) ligand 2
Cd14, CD14 antigen
Cd36, CD36 antigen (fatty acid translocase)
Col1a1, collagen, type I, alpha 1
Cybb, cytochrome b-245, beta polypeptide
Ddit3, DNA-damage inducible transcript 3
Dgat1, diacylglycerol O-acyltransferase 1
Dgat2, diacylglycerol O-acyltransferase 2

Fabp1, fatty acid binding protein 1, liver
Fasn, fatty acid synthase
Gpx1, glutathione peroxidase 1
Il1b, interleukin 1 beta
Lipe, hormone-sensitive lipase
Mttp, microsomal triglyceride transfer protein
Myd88, myeloid differentiation primary response gene 88
Ncf1, neutrophil cytosolic factor 1
Nlrp3, NLR family, pyrin domain containing 3
Nlrp4, NLR family, pyrin domain containing 4
Pnpla2, patatin-like phospholipase domain containing 2 (adipose triglyceride lipase)
Pycard, PYD and CARD domain containing
Sod1, superoxide dismutase 1, soluble
Spp1, secreted phosphoprotein 1 (osteopontin)
Tnf, tumor necrosis factor alpha
Tlr2, toll-like receptor 2
Tlr4, toll-like receptor 4